

Spectral properties of Antarctic and Alpine vegetation monitored by multispectral camera: Case studies from James Ross Island and Jeseníky Mts.

Peter Váczi^{1*}, Miloš Barták¹, Michaela Bednaříková¹, Filip Hrbáček², Josef Hájek¹

¹Laboratory of Photosynthetic Processes, Department of Experimental Biology, Faculty of Science, Masaryk University, Kamenice 5, 625 00 Brno, Czech Republic

²Polar-Geo-Lab, Department of Geography, Faculty of Science, Masaryk University, Kotlářská 2, 611 37, Brno, Czech Republic

Abstract

In this study, we investigated the utility of spectral remote sensing data gathered by a multispectral camera for estimating of vegetation cover in Antarctic vegetation oasis and Arcto-Alpine tundra. The surveys exploiting unmanned aerial vehicles (UAV) and multispectral camera were done in an Antarctic vegetation oasis located at the Northern shore of James Ross Island (Antarctica), and arcto-alpine tundra located in the Jeseníky Mts. (NE Czech Republic, 1 420 m a.s.l.). For the two locations, false colour images of spectral indices (VARI, NGRDI, GLI, RGBVI, ExG, NDVI, PRI) were taken and analysis of vegetation types and components of vegetation cover was done. Additionally, field research was performed by handheld instruments measuring NDVI, PRI and of selected vegetation components: *Bryum pseudotriquetrum*, *Nostoc commune* colonies (Antarctica), lichens grown on flat stones and boulders (the Jeseníky Mts.). The results show UAV photo surveys and imaging of spectral reflectance indices can be used to monitor vegetation types forming Antarctic vegetation oases and arcto-alpine tundra.

Key words: remote sensing, UAV, vegetation indices, spectral reflectance, plant functional types

DOI: 10.5817/CPR2020-2-22

Symbols and abbreviations: LTRP – Long-Term Research Plot (on James Ross Island), NDVI – Normalized Difference Vegetation Index, PRI – Photochemical Reflectance Index, VARI – Visible Atmospheric Resistant Index, NGRDI – Normalized Green-Red Difference Index, GLI – Green Leaf Index, RGBVI – Red-Green-Blue Vegetation Index, ExG – Normalized Excess Green Index, R – red, G – green, B – blue

Received July 30, 2020, accepted December 30, 2020.

*Corresponding author: P. Váczi <vaczi@sci.muni.cz>

Acknowledgements: The study reported in this paper was supported by the ECOPOLARIS project (CZ.02.1.01/0.0/0.0/ 16_013/0001708) provided by the Czech Ministry of Education, Youth, and Sports. The authors are grateful to the CzechPolar2 (LM2015078) for the possibility to use laboratory infrastructure MBa and JHa are indebted to the ARCTOS MU project for support. Computational resources were supplied by the project "e-Infrastruktura CZ" (e-INFRA LM2018140) provided within the program Projects of Large Research, Development and Innovations Infrastructures.

Introduction

Remote sensing provides an opportunity to monitor vegetation cover at a great variety of spatial and temporal scales in Arctic (Stow *et al.* 2004), Antarctica (Jawak *et al.* 2019, Gaffey *et al.* 2020), and Alpine environments (Duan *et al.* 2011). In last decades, several vegetation indices have been successfully tested in treeless polar and alpine environments to distinguish components of their vegetation cover (*see* Beamish *et al.* 2020 for review). Among them, the Normalized Difference Vegetation Index (NDVI) has been applied to characterize different types of vegetation types forming vegetation cover and their vigour. However, in the ecosystems with partial or full absence of vascular plants, NDVI evaluation is rather complicated because of species-specific optical properties and spectral signature of mosses, lichens (Barták *et al.* 2018) and cyanobacteria. However, Casanovas *et al.* (2015) compared NDVI and matched filtering approaches for mapping lichens in Antarctica.

Recently, unmanned aerial vehicles (UAV) and 'on board' spectral cameras are used in Antarctica for vegetation mapping using an either visible or broad-band multispectral approach in moss beds in the majority of cases (Lucieer *et al.* 2010, 2012; Turner *et al.* 2014, 2018). Moreover, other types of vegetation cover, such as, *e.g.* microbiological mats, are distinguished

by UAV as well (Levy *et al.* 2020). Even during the summer period, these organisms are exposed to low temperature, strong wind, high irradiance and other stressors. Among them, limited liquid water availability plays an important role, so that Antarctic vegetation passes through several dehydration and rehydration events during the austral summer season. All the above-specified environmental stressors may influence the photosynthetic performance as well as spectral reflectance properties of photosynthesizing organisms. Therefore, spectral reflectance is a beneficial method for analyzing different types of vegetation both by ground and remote sensing approach. The most commonly used spectral reflectance indices are the NDVI (associated with the chlorophyll content and dehydration in lichens), and PRI (photochemical reflectance index, related to the xanthophyll cycle conversion and changes in PSII functioning).

In this study, we used UAV equipped with a spectral camera to classify vegetation types of Antarctic vegetation oasis (James Ross Island, Antarctica) and arcto-alpine tundra in the Jeseníky Mts. We hypothesized that spectral indices would be sufficient tool to distinguish fine-scale differences in dominant species forming patchy spots in vegetation cover of the two experimental sites.

Material and Methods

In this study, two areas were investigated by UAV-carried spectral camera: (1) vegetation oasis at James Ross Island, Antarctica, and (2) arcto-alpine tundra vegeta-

tion neighbouring rocky outgrowth (the Jeseníky Mountains ridge, NE Czech Republic).

Description of Antarctic vegetation oasis

In this paper, we focused on spectral properties of vegetation cover constituents forming vegetation oasis at a coastal ter-

race (63° 48' 00" S, 57° 52' 56" W, 6 m a. s. l.) of the northern coast of James Ross Island. The vegetation oasis is a part of a

long-term research plot (LTRP) that was established in January 2007 in the neighbourhood of the Czech station (J. G. Mendel). The LTRP is located close to a coastal line in between the confluxes of the Bohemian and Algal streams. The area is dominated by *Bryum pseudotriquetrum* that forms carpets, a longitudinal axis that follows the line of thawing water pathway from a temporary snowfield located hillside 50 m away from the area. The area

comprises two subareas and rich in microbial mats formed by *Nostoc* sp. colony, algal (*e.g. Zygnema* sp.) and cyanobacterial species at the bottom of shallow streams vegetatively active for a short-term period during austral summer (Komárek 2013, Komárek et al. 2015). Out of moss carpet area, a stony surface is covered by patches of lichens, such as *e.g. Rhizoplaca melanophthalma*, *Xanthoria elegans* (Barták et al. 2015)

Description of arcto-alpine tundra

The area under investigation is the Tabulové skály rocks (50° 5' 15.398" N, 17° 13' 52.435" E). The site is a forest-free area located at the altitude of 1420 m a.s.l. (the Jeseníky Mts. NE of the Czech Republic). The rocky outgrowths are surrounded by alpine plant communities classified as wind-swept alpine grasslands and closed alpine grasslands (Nardo-Caricion

rigidae). In the Tabulové skály rocks neighbourhood, non-native *Pinus mugo* stands are found (for more detail see Barták et al. in this CPR issue). The Tabulové skály rocks is a locality rich in lichen and moss flora with some glacial relicts of vascular plants, such as *e.g. Salix herbacea*, that grows mainly along the rock edges.

Aerial vegetation images and data processing

The long-term research plot vegetation images were acquired by using UAV Phantom 3 (DJI, Shenzhen, China) equipped with RGB camera in about 20 m above ground level within one flight at stable light condition. The vegetation images of Tabulové skály rocks area were taken using UAV Matrice 200 (DJI, Shenzhen, China) equipped with multispectral Red Edge-M camera (Micasense Inc., USA) in height of 20 m above ground level within one flight at the stable light condition. Additionally, the reference images of calibration reflectance panel (Micasense Inc., USA) were acquired immediately before and after flight for radiometric calibration of multispectral images.

The acquired image data were processed using the structure from motion photogrammetry software Agisoft Metashape Professional v. 1.6 (Agisoft LLC.) to derive a multichannel orthomosaic with 1.8 cm

spatial resolution. Spectral indices were calculated per plot from the multispectral camera's narrow-band spectral images (Red Edge-M, for the Jeseníky Mts). Additional parameters were calculated from red (R, 586-608 nm), green (G, 545-575 nm), and blue (B, 439-455 nm) colour channels (RGB camera, for the LTRP). Several spectral indices were calculated for each image pixel and visualized in false colour scale (see Table 1, and Figs. 1-2, 4-6). The images were used for the analysis of constituents of vegetation cover and characteristics of vegetation-free areas as well as the physiological status of particular plant species. For analysis of spectral indices at James Ross Island, the following covers were distinguished: bare soil (sites 7-8; Fig. 1), regolith, microbiological soil crusts, moss carpets (sites 1-6, 11-12), and *Nostoc commune* colonies (sites 3-6, 9-10; Fig. 1) in seepages. For the Jeseníky Mts. area, the

following types of cover were used (*see* Fig. 4): (A) vegetation-free stony field, (B) *Vaccinium myrtillus*-dominated stand, (C) *Nardus stricta*-dominated arcto-alpine grass, (D) *Pinus mugo* stand, (E) alpine meadows rich in vascular plant species, and (F) moss-carpet covering stony places.

Index	Equation	Reference
Visible Atmospheric Resistant Index	$VARI = \frac{R_G - R_R}{R_G + R_R - R_B}$	Gitelson <i>et al.</i> 2002
Normalized Green-Red Difference Index	$NGRDI = \frac{R_G - R_R}{R_G + R_R}$	Tucker 1979
Green Leaf Index	$GLI = \frac{2 \times R_G - R_R - R_B}{2 \times R_G + R_R + R_B}$	Louhaichi <i>et al.</i> 2001
Triangular Greenness Index	$TGI = R_G - 0.39 \times R_R - 0.61 \times R_B$	Hunt <i>et al.</i> 2013
Red-Green-Blue Vegetation Index	$RGBVI = \frac{R_G^2 - R_R \times R_B}{R_G^2 + R_R \times R_B}$	Bendig <i>et al.</i> 2015
Normalized Excess Green Index	$ExG = \frac{2 \times R_G - R_R - R_B}{R_G + R_R + R_B}$	Woebbecke <i>et al.</i> 1995
Normalized Difference Vegetation Index	$NDVI = \frac{R_{NIR} - R_R}{R_{NIR} + R_R}$	Rouse <i>et al.</i> 1974
Modified Simple Ratio Index	$MSR = \frac{R_{NIR}/R_R - 1}{\sqrt{R_{NIR}/R_R + 1}}$	Chen 1996
Green Chlorophyll Index	$CI_{green} = \frac{R_{NIR}}{R_G} - 1$	Gitelson <i>et al.</i> 2003
Photochemical Reflectance Index	$PRI = \frac{(R_{531} - R_{570})}{(R_{531} + R_{570})}$	Gamon <i>et al.</i> 1992

Table 1. Overview of applied vegetation reflectance indices calculated from RGB and narrow-band reflectance data.

Spectral measurements by handheld instrument

In 2018 austral summer season, we measured spectral reflectance curves (380–800 nm) at the LTRP (James Ross Island, Antarctica), using a PolyPen RP 400 (Photon System Instruments, Czech Republic). Several reflectance indices were analyzed (*see* Table 1). The measurements were done repeatedly in 3–4 days intervals. Afterwards, we compared mean values of in-

indices for vegetation types concerning the local weather conditions (temperature and humidity). The vegetation types were: (A) *Bryum pseudotriquetrum*-dominated moss carpet (sites 1–6, and 11–12 in Figs. 1 and 2), (B) colonies of *Nostoc commune* (sites 3–6 and 9–10), (C) bare soil (sites 7–8), and (D) biological soil crusts formed by several algal/lichen/moss species.

In summer season 2019, spectral reflectance curves (380-800 nm) were measured on Tabulové skály rocks. The same instrument (PolyPen RP 400) was used for the analysis of reflectance indices. Measured vegetation types were: (A) vegetation-free

stony field, (B) *Vaccinium myrtillus*-dominated stand, (C) *Nardus stricta*-dominated arcto-alpine grass, (D) *Pinus mugo* stand, (E) alpine meadows rich in vascular plant species, and (F) moss-carpet covering stony places (Fig. 4).

Results and Discussion

For Antarctic vegetation oasis, PRI, NDVI, GLI, RGBVI, and EXG indices showed they are very sensitive in the indication of moss-dominated vegetation cover (see Figs. 1, 2). The other vegetation oasis components, such as seepages, biological soil crusts and lichen-dominated sites are less distinguishable. However, the bottom of the seasonal stream (fed by a melting snowfield during austral summer) covered by a thin surface-attached community of algae and cyanobacteria when hydrated can be easily distinguished from surrounding bare soil and stony regolith (see localities 9 and 10 in Fig. 1, 2). This is well comparable to the evidence of seasonal algal bloom monitoring and biomass estimation reported by Gray et al. (2020). It can be concluded that the spectral indices used in our study might be applied for the evaluation of plant functional types in Antarctic vegetation oases and follow-up vegetation classification studies. For lichen-dominated vegetation cover, however, more basic research is needed to distinguish particular species groups and, possibly, their physiological status, *i.e.* physiological functioning when wet and physiological dormancy when dry. The approach is prospective for evaluating spatial distribution, spectral properties and temporal variability of primary producers of Antarctic terrestrial vegetation oasis, as shown, *e.g.* by Salvatore et al. (2020) for Dry Valleys. However, small-scale analysis of remote spectral data in lichen vegetation cover seems to be still problematic. With re-

cent technologies, the approach could be applied only for relatively large spots (the area of hundreds of square cm) with mono-specific lichen cover.

The apparent colour of Antarctic cryptogamic vegetation, largely consisting of lichens, depends on the amount and chemical structure protective compound allocated in the upper cortex, and hydration state which changes the optical properties of lichen thalli. Therefore, additional multi-spectral bands, *e.g.* near infra-red indices, rather than the more traditional visible-near infrared bands seem to be better for detecting this type of vegetation, as suggested by *e.g.* by Calviño-Cancela and Martín-Herrero (2015) and Jawak et al. (2019). For follow-up remote sensing studies in lichen-dominated polar vegetation, the identification of mosses and lichens, and the definition of their spectral properties are critical requirements for improving vegetation remote sensing and evaluation of polar tundra plant functional types. For moss-dominated vegetation oasis, Turner et al. (2018) suggested a combined approach of spectral reflectance-based remote imaging and modelling in order to evaluate health status of Antarctic moss cushions. Moreover, spectral properties of plant functional types can be related to light use efficiency (LUE) as reported for tundra vegetation components by *e.g.* Huemmrich et al. (2013). The latter approach has a great potential for follow-up studies in polar regions.

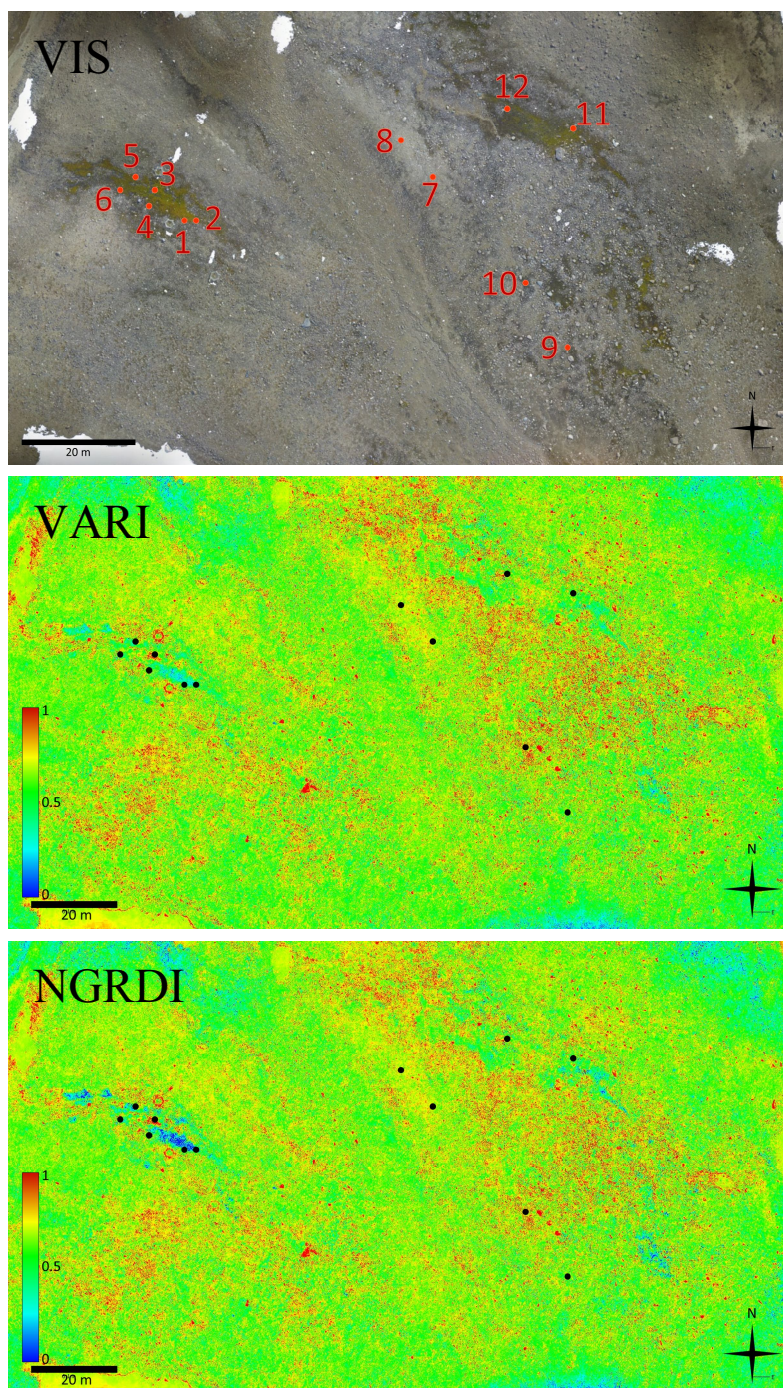


Fig. 1. Visual (VIS) and false colour images of VARI, NGRDI indices distribution on long-term research plot (LTRP), James Ross Island, with the points of measurements of vegetation types. Hexagonal structures close to '1' and '3' in the VIS image are OTCs installed at the LTRP in 2007.

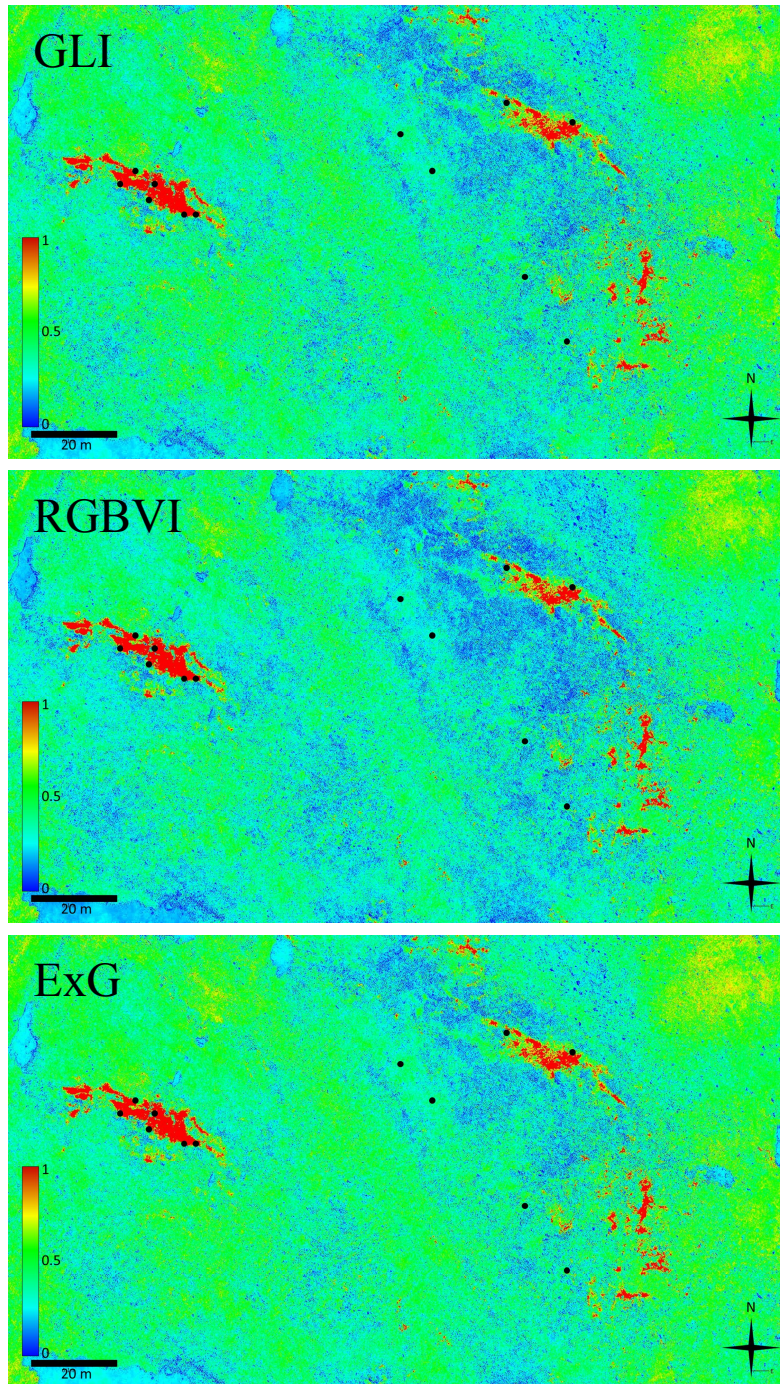


Fig. 2. False colour images of GLI, RGBVI, ExG indices distribution on long-term research plot (LTRP), James Ross Island, Antarctica, with highlighted localities of different measured vegetation types (compare with Fig. 1).

Site No. – species (status)	NDVI	PRI	VARI	NGRDI	GLI	TGI	RGBVI	ExG
1 – <i>Bryum</i> (wet)	0.729 ±0.105	-0.164 ±0.03	-0.003 ±0.043	-0.003 ±0.036	0.213 ±0.031	0.626 ±0.35	0.548 ±0.057	0.306 ±0.048
2 – <i>Bryum</i> (medium wet)	0.589 ±0.075	-0.137 ±0.023	-0.036 ±0.033	-0.030 ±0.027	0.182 ±0.03	0.595 ±0.139	0.489 ±0.06	0.259 ±0.045
3a – <i>Bryum</i> (wet)	0.763 ±0.152	-0.142 ±0.031	0.016 ±0.03	0.013 ±0.025	0.196 ±0.042	0.393 ±0.136	0.469 ±0.095	0.280 ±0.064
3b – <i>Nostoc</i> (wet)	0.321 ±0.107	-0.045 ±0.014	-0.025 ±0.036	-0.013 ±0.015	0.025 ±0.031	0.039 ±0.169	0.053 ±0.064	0.033 ±0.041
4a – <i>Bryum</i> (medium wet)	0.616 ±0.087	-0.174 ±0.018	-0.050 ±0.023	-0.041 ±0.018	0.163 ±0.034	0.427 ±0.143	0.445 ±0.084	0.231 ±0.051
4b – <i>Nostoc</i> (medium wet)	0.400 ±0.103	-0.064 ±0.019	-0.031 ±0.012	-0.019 ±0.008	0.053 ±0.03	0.085 ±0.051	0.119 ±0.07	0.072 ±0.041
5a – <i>Bryum</i> (wet)	0.686 ±0.12	-0.086 ±0.024	0.018 ±0.031	0.014 ±0.025	0.133 ±0.038	0.265 ±0.076	0.298 ±0.13	0.187 ±0.086
5b – <i>Nostoc</i> (wet)	0.279 ±0.121	-0.039 ±0.021	-0.022 ±0.024	-0.012 ±0.012	0.019 ±0.024	0.033 ±0.089	0.042 ±0.05	0.026 ±0.032
6a – <i>Bryum</i> (medium wet)	0.650 ±0.09	-0.162 ±0.024	-0.045 ±0.019	-0.036 ±0.016	0.156 ±0.032	0.423 ±0.104	0.415 ±0.087	0.219 ±0.047
6b – <i>Nostoc</i> (medium wet)	0.368 ±0.067	-0.053 ±0.011	-0.050 ±0.066	-0.022 ±0.016	0.020 ±0.057	-0.012 ±0.384	0.049 ±0.11	0.029 ±0.073
7 – bare soil wet	0.130 ±0.006	-0.083 ±0.007	-0.076 ±0.004	-0.054 ±0.003	0.078 ±0.003	0.519 ±0.135	0.202 ±0.01	0.107 ±0.005
8 – bare soil medium wet	0.125 ±0.012	-0.076 ±0.007	-0.074 ±0.006	-0.052 ±0.005	0.071 ±0.007	0.452 ±0.121	0.181 ±0.022	0.097 ±0.01
9 – <i>Nostoc</i> (wet)	0.290 ±0.065	-0.062 ±0.022	-0.046 ±0.044	-0.026 ±0.016	0.035 ±0.036	0.096 ±0.18	0.082 ±0.072	0.048 ±0.046
10 – <i>Nostoc</i> (medium wet)	0.359 ±0.031	-0.088 ±0.031	-0.060 ±0.023	-0.040 ±0.017	0.044 ±0.013	0.142 ±0.063	0.108 ±0.035	0.060 ±0.018
11 – <i>Bryum</i> (wet)	0.806 ±0.036	-0.164 ±0.022	0.010 ±0.04	0.009 ±0.033	0.212 ±0.043	0.435 ±0.137	0.521 ±0.089	0.304 ±0.066
12 – <i>Bryum</i> (dead)	0.213 ±0.055	-0.046 ±0.01	-0.043 ±0.008	-0.026 ±0.005	0.037 ±0.006	0.094 ±0.039	0.083 ±0.013	0.050 ±0.008

Table 2. Values of analyzed reflectance indices for particular components of vegetation cover recorded during austral summer 2018. The sites are numbered 1–12 (for locations of the sites in the Antarctic vegetation oasis at the long-term research plot, James Ross Island, see Fig. 1). *Bryum – Bryum pseudotriquetrum*, *Nostoc – Nostoc commune*. Values are means ± standard deviation.

Field measurements of PRI, NDVI, and other reflectance indices for the LTRP at James Ross Island (Antarctica) revealed a small seasonal dynamics dependent on microclimate, liquid water availability in particular. Typically, PRI and NDVI changed from medium wet to dry state in the autotrophs reported in Table 2.

The results gained at the vegetation oasis (James Ross island) suggest that photosynthesizing communities forming the oasis can be detected by remote sensing and *in situ* measurements using spectral reflectance indices. Intra- and inter-annual variability in spectral signatures might be attributed to short-term variations in their distribution (biological mats especially), their

hydration status and photosynthetic activity in response to hydration. Numeric value of particular spectral reflectance indices in poikilohydric mosses and lichens are dependent on their hydration status as shown earlier in laboratory studies (Barták et al. 2018). In the field Antarctic studies, the measurements of lichen thallus and/or moss cushion hydration status, however, meet some difficulties due to technical problems with installations of sensors into a moss and/or lichen thalli. In spite of that, future studies combining remote sensing of spectral characteristics of Antarctic vegetation with *in situ* measurements of physical environment variables seems to be a promising approach.

Tabulové skály rocks

The arcto-alpine tundra components at the Tabulové skály rocks were well distinguishable both in visual UAV photography and the false colour images of VARI, NGRDI, GLI, RGBVI, ExG, NDVI, PRI (Fig. 4-6). Significant components (rocks, stony fields, boulders) and vegetation types (*Vaccinium myrtillus*, *Pinus mugo*, alpine meadows stands, *Nardus stricta*-dominated grass stand) were identified on the false colour images of the indices. These vegetation components formed relatively dense, homogeneous patches. The results of this study show that, similarly to recent studies

(e.g. Fraser et al. 2016, Siewert and Olofsson 2020), UAV photo surveys can be used to monitor vegetation types forming arcto-alpine tundra and the changes in fine-scale vegetation composition. Moreover, season-related changes in greenness pattern for particular vegetation type could be monitored if repeated surveys (UAV flights) are done within a single season. This is valid e.g. for *Empetrum* sp. that showed bright orange-brown foliage after the winter of 2019/2020 followed by gradually developing green foliage in mid-summer season (see Fig. 3).

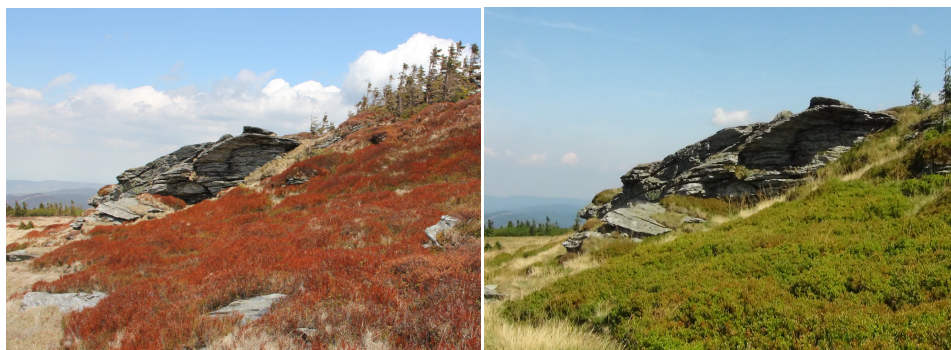


Fig. 3. Early spring (left) and summer view (right) on *Vaccinium myrtillus*-dominated patchy stands (Tabulové skály rocks).

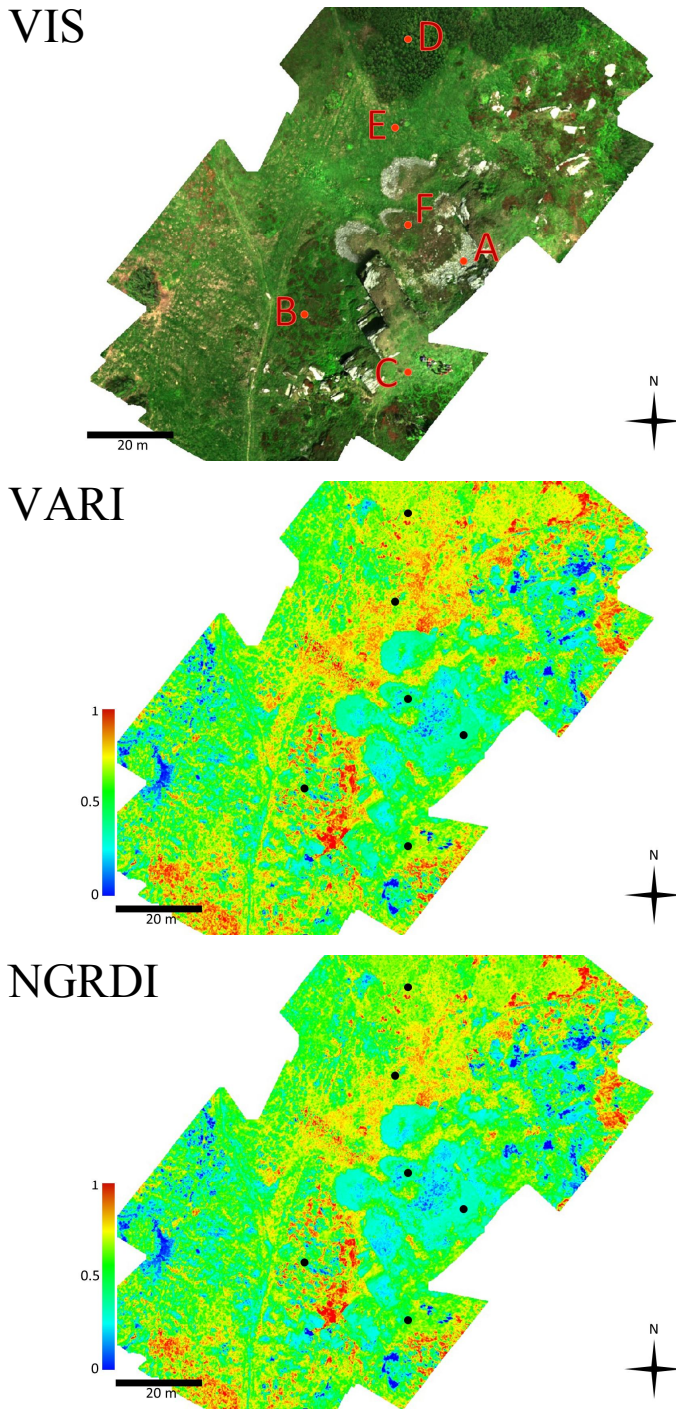


Fig. 4. Visual (VIS) and false colour images of VARI, and NGRDI indices in Tabulové skály locality with highlighted sites: (A) vegetation-free stony field; (B) *Vaccinium myrtillus*-dominated stand; (C) *Nardus stricta*-dominated arcto-alpine grass; (D) *Pinus mugo* stand; (E) alpine meadows; (F) moss-carpet over stony places.

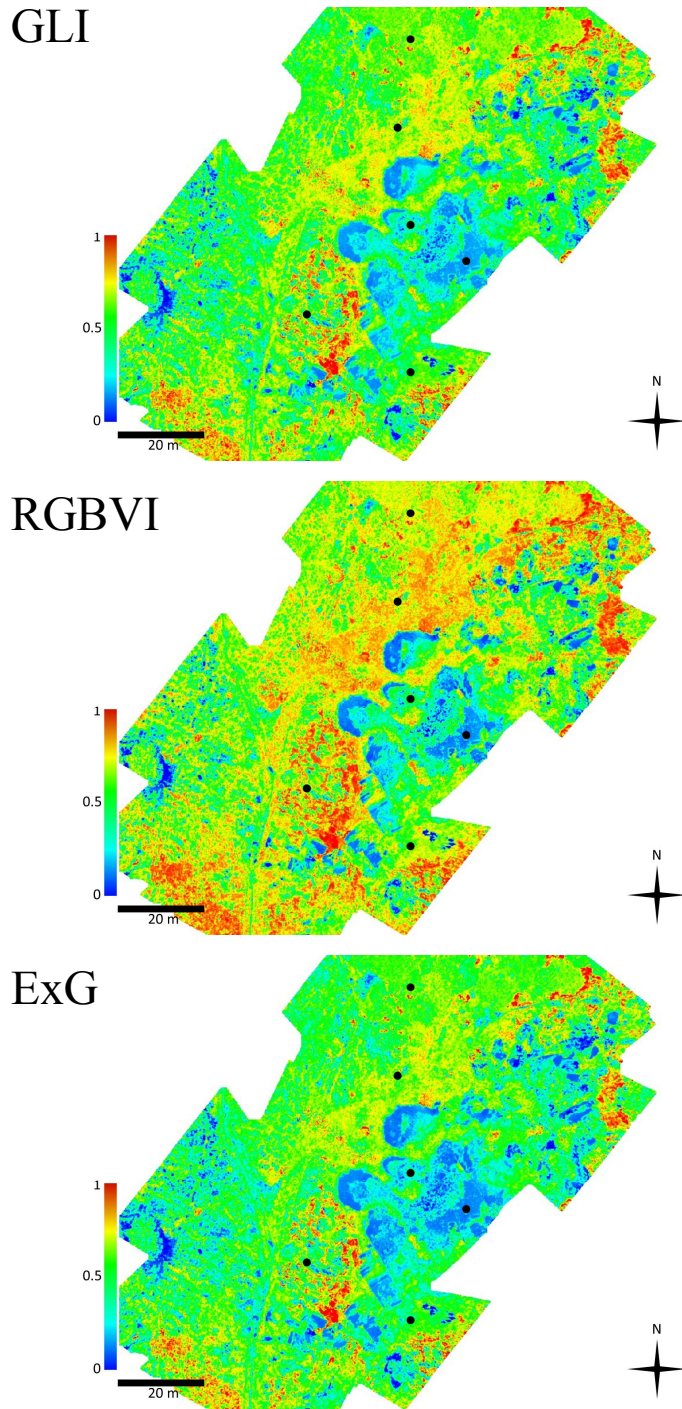


Fig. 5. False colour images of GLI / RGBVI / ExG indices distribution on Tabulové skály rocks locality with highlighted different measured vegetation types (compare with Fig. 4).

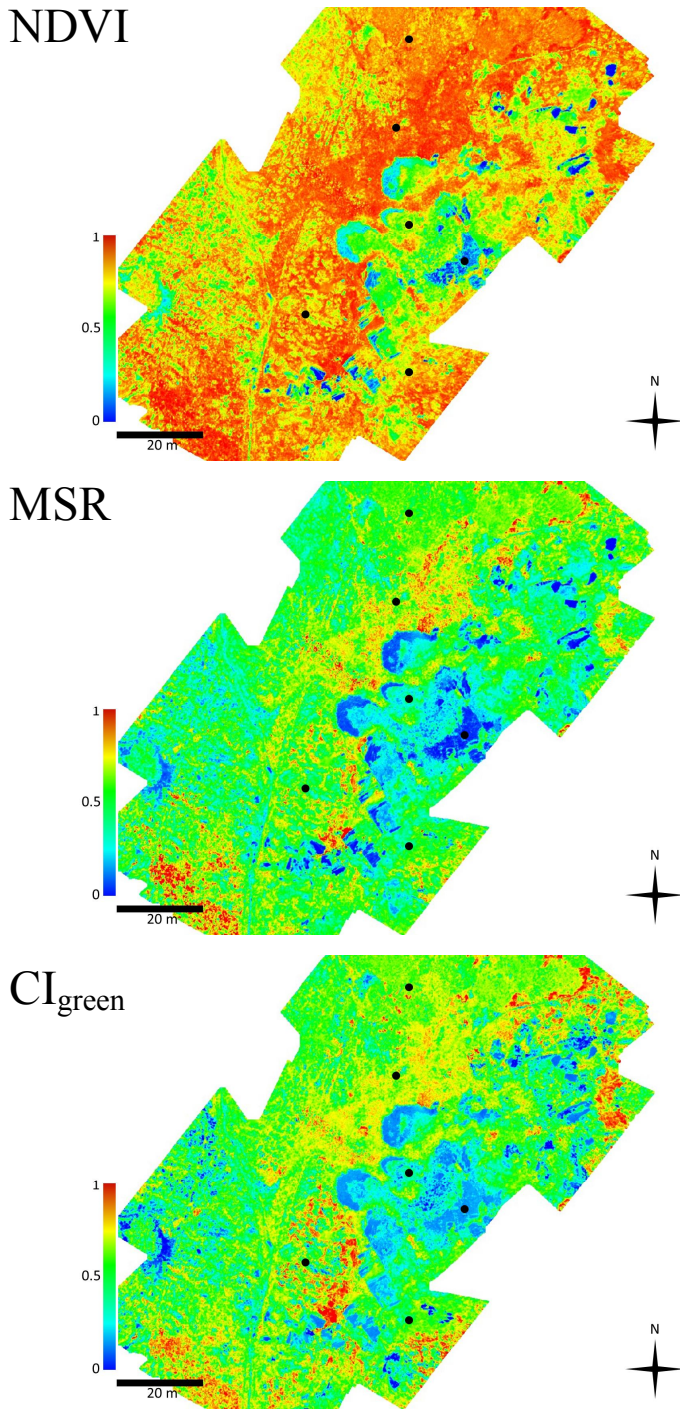


Fig. 6. False colour images of NDVI, MSR, and CI_{green} indices distribution on Tabulové skály rocks locality with highlighted different measured vegetation types (compare with Fig. 4).

Site No. – species	VARI	NGRDI	GLI	TGI	RGBVI	EXG	NDVI	PRI
Lichen white thallus	-0.005 ±0.004	-0.003 ±0.002	0.011 ±0.006	0.006 ±0.004	0.021 ±0.013	0.014 ±0.008	0.218 ±0.022	-0.017 ±0.002
<i>Rhizocarpon</i>	-0.003 ±0.004	-0.002 ±0.003	0.209 ±0.018	0.132 ±0.03	0.533 ±0.054	0.300 ±0.027	0.108 ±0.017	-0.013 ±0.004
Moss <i>Sphagnum</i> sp.	-0.002 ±0.014	-0.001 ±0.011	0.170 ±0.015	0.060 ±0.019	0.410 ±0.035	0.240 ±0.023	0.390 ±0.066	-0.075 ±0.012
Grass stand	0.139 ±0.04	0.096 ±0.033	0.177 ±0.049	0.027 ±0.004	0.356 ±0.095	0.252 ±0.076	0.765 ±0.058	0.028 ±0.019
Lichen <i>Umbilicaria</i> sp.	-0.054 ±0.007	-0.030 ±0.004	0.007 ±0.006	0.001 ±0	0.017 ±0.012	0.010 ±0.007	0.272 ±0.042	-0.028 ±0.029
Lichen yellow thallus	-0.005 ±0.04	-0.005 ±0.025	0.134 ±0.045	0.065 ±0.031	0.323 ±0.12	0.188 ±0.065	0.137 ±0.035	-0.022 ±0.025
Bare rock	-0.003 0.0022	-0.002 0.0012	0.023 0.0009	0.012 0.0004	0.046 0.0017	0.030 0.0012	-0.007 0.0009	0.013 0.007

Table 3. Values of analyzed reflectance indices measured on epilithic lichens of different thali colour and several components of vegetation cover by handheld instruments at the Tabulové skály rocks. Values are means ± standard deviation.

Individual boulders with flat horizontally-arranged upper surfaces were found at the top and bottom parts of the images and indicated by the blue colour in false colour images (white in visible). Field measure-

ments of reflectance indices were done in spots dominated by differently coloured lichen species for these boulders. Even though for lichens, numeric values are hydration status-dependent (Singh et al. 2013, Barták et al. 2018), indices showed lichen species specificity according to thallus colour (Table 3).

From selected indices, RGBVI, derived from RGB visual image analysis, showed a high dynamic range that can help distinguish different community forming species and plant functional types and comprise biotic cover in alpine ecosystems. The RGVBI might be recommended for the studies done in early-stage biotic cover as well as, e.g. freshly deglaciated fields in maritime Antarctica. NDVI, however, as a narrow-band spectral analysis index might be correlated with the degree of active chlorophyll composition in analyzed biocover in both field plots. Therefore, NDVI should be used preferably in the studies focused on metabolic/physiological activity of vegetation component and their coverage area. It is because of the fact that some cryptogamic species exhibit low reflectance in the near-infrared region and are not easily detected by NDVI (Sotille et al. 2020). This may complicate NDVI-based determination of species or vegetation functional groups (e.g. in lichens). Additionally, the spectral reflectance of cryptogamic Antarctic vegetation is highly variable according to water contents and seasonal conditions that influence NDVI value. In lichens, thanks to secondary pigments other than chlorophyll, the red edge is usually absent or very weak on spectral reflectance curve. This explains the lower ability of NDVI to distinguish different lichen species in Antarctica (Fretwell et al. 2011, Casanovas et al. 2015). In the lichen species with black thalli (e.g. genera *Psoroma* and *Himantormia*), extremely low reflectance in the visible wavelengths is found which limits the use of NDVI in such lichen species.

References

- BARTÁK, M., VÁCZI, P., STACHOŇ, Z. and KUBEŠOVÁ, S. (2015): Vegetation mapping of moss-dominated areas of northern part of James Ross Island (Antarctica) and a suggestion of protective measures. *Czech Polar Reports*, 5: 75-87.
- BARTÁK, M., HÁJEK, J., MORKUSOVÁ, J., SKÁCELOVÁ, K. and KOŠUTHOVÁ, A. (2018): Dehydration-induced changes in spectral reflectance indices and chlorophyll fluorescence of Antarctic lichens with different thallus color, and intrathalline photobiont. *Acta Physiologiae Plantarum*, 40: 177. doi: 10.1007/s11738-018-2751-3.
- BARTÁK, M., OREKHOVA, A., NEZVAL, J., ORAVEC, M., HÁJEK, J., ŠPUNDA, V., TRÍSKA, J., BEDNÁŘIKOVÁ, M., GIUDICI, G. N. M. and PECH, R. (2020, in this CPR issue): Light regimen-induced variability of photosynthetic pigments and UV-B absorbing compounds in *Luzula sylvatica* from arcto-alpine tundra. *Czech Polar Reports*, 10(2): 263-280.
- BEAMISH, A., RAYNOLDS, M. K., EPSTEIN, H., FROST, G. V., MACANDER, M. J., BERGSTEDT, H., BARTSCH, A., KRUSE, S., MILES, V., TANIS, C. M., HEIM, B., FUCHS, M., CHABRILLAT, S., SHEVTSOVA, I., VERDONEN, M. and WAGNER, J. (2020): Recent trends and remaining challenges for optical remote sensing of Arctic tundra vegetation: A review and outlook. *Remote Sensing of Environment*, 246: 111872. doi: 10.1016/j.rse.2020.111872
- BENDIG, J., YU, K., AASEN, H., BOLTEN, A., BENNERTZ, S., BROSCHEIT, J., GNYP, M. L. and BARETH, G. (2015): Combining UAV-based plant height from crop surface models, visible, and near infrared vegetation indices for biomass monitoring in barley. *International Journal of Applied Earth Observation and Geoinformation*, 39: 79-87.
- CALVIÑO-CANCELA, M., MARTÍN-HERRERO, J. (2016): Spectral discrimination of vegetation classes in ice-free areas of Antarctica. *Remote Sensing*, 8: 856. doi: 10.3390/rs8100856
- CASANOVAS, P., BLACK, M., FRETWELL, P. and CONVEY, P. (2015): Mapping lichen distribution on the Antarctic Peninsula using remote sensing, lichen spectra and photographic documentation by citizen scientists. *Polar Research*, 34: 25633.
- CHEN, J. M. (1996): Evaluation of vegetation indices and a modified simple ratio for boreal applications. *Canadian Journal of Remote Sensing*, 22(3): 229-242. doi: 10.1080/07038992.1996.10855178
- DUAN, M., GAO, Q., WAN, Y., LI, Y., GUO, Y., GANZHU, Z., LIU, Y. and QIN, X. (2011): Biomass estimation of alpine grasslands under different grazing intensities using spectral vegetation indices. *Canadian Journal of Remote Sensing*, 37(4): 413-421. doi: 10.5589/m11-050.
- FRASER, R. H., OLTHOF, I., LANTZ, T. C. and SCHMITT, C. (2016): UAV photogrammetry for mapping vegetation in the low-Arctic. *Arctic Science*, 2(3): 79-102. doi: 10.1139/as-2016-0008.
- FRETWELL, P. T., CONVEY, P., FLEMING, A. H., PEAT, H. J. and HUGHES, K. A. (2011): Detecting and mapping vegetation distribution on the Antarctic Peninsula from remote sensing data. *Polar Biology*, 34: 273-281.
- GAFFEY, C., BHARDWAJ, A. (2020): Applications of unmanned aerial vehicles in cryosphere: Latest advances and prospects. *Remote Sensing*, 12: 948.
- GAMON, J. A., PEÑUELAS, J. and FIELD, C. B. (1992): A narrow-waveband spectral index that tracks diurnal changes in photosynthetic efficiency. *Remote Sensing of Environment*, 41: 35-44.
- GITELSON, A. A., GRITZ, Y. and MERZLYAK, M. N. (2003): Relationships between leaf chlorophyll content and spectral reflectance and algorithms for non-destructive chlorophyll assessment in higher plant leaves. *Journal of Plant Physiology*, 160: 271-282.
- GRAY, A., KROLIKOWSKI, M., FRETWELL, P., CONVEY, P., PECK, L. S., MENDELOVA, M., SMITH, A. G. and DAVEY, M. P. (2020): Remote sensing reveals Antarctic green snow algae as important terrestrial carbon sink. *Nature Communications*, 11: 2527.
- HUNT, E. R., DORAISWAMY, P. C., MCMURTREY, J. E., DAUGHTRY, C. S. T., PERRY, E. M. and AKHMEDOV, B. (2013): A visible band index for remote sensing leaf chlorophyll content at the canopy scale. *International Journal of Applied Earth Observation and Geoinformation*, 21: 103-112.

- HUEMMRICH, K. F., GAMON, J. A., TWEEDIE, C. E., CAMPBELL, P. K. E., LANDIS, D. R. and Middleton, E. M. (2013): Arctic tundra vegetation functional types based on photosynthetic physiology and optical properties. *IEEE Journal of Selected Topics in Applied Earth Observations and Remote Sensing*, 6(2): 265-275. doi: 10.1109/JSTARS.2013.2253446.
- JAWAK, S. D., LUIS, A. J., FRETWELL, P. T., CONVEY, P. and DURAIRAJAN, U. A. (2019): Semiautomated detection and mapping of vegetation distribution in the Antarctic environment using spatial-spectral characteristics of WorldView-2 Imagery. *Remote Sensing*, 11: 1909.
- KOMÁREK, J. (2013): Phenotypic and ecological diversity of freshwater coccoid cyanobacteria from maritime Antarctica and islands of NW Weddell Sea. I. Synechococcales. *Czech Polar Reports*, 3(2): 130-143.
- KOMÁREK, J., GENUÁRIO, D. B., FIORE, M. F. and ELSTER, J. (2015): Heterocytous cyanobacteria of the Ulu Peninsula, James Ross Island, Antarctica. *Polar Biology*, 38: 475-492. doi: 10.1007/s00300-014-1609-4.
- LEVY, J., CARY, S., JOY, K. and Lee, C. (2020): Detection and community-level identification of microbial mats in the McMurdo Dry Valleys using drone-based hyperspectral reflectance imaging. *Antarctic Science*, 32(5): 367-381. doi:10.1017/S0954102020000243
- LOUHAICHI, M., BORMAN, M. M. and JOHNSON, D. E. (2001): Spatially located platform and aerial photography for documentation of grazing impacts on wheat. *Geocarto International*, 16: 65-70.
- LUCIEER, A., ROBINSON, S., TURNER, D., HARWIN, S. and KELCEY, J. (2012): Using a micro-UAV for ultra-high resolution multi-sensor observations of antarctic moss beds. International Archives of the Photogrammetry, Remote Sensing and Spatial Information Sciences, Volume XXXIX-B1, 2012 XXII ISPRS Congress, 25 August – 01 September 2012, Melbourne, Australia. pp. 429–433. <https://doi.org/10.5194/isprsarchives-XXXIX-B1-429-2012>
- LUCIEER, A., ROBINSON, S. and TURNER, D. (2011): Unmanned aerial vehicle (UAV) remote sensing for hyperspatial terrain mapping of Antarctic moss beds based on structure from motion (SfM) point clouds. Proceedings of the 34th International Symposium on Remote Sensing of Environment - The GEOSS Era: Towards Operational Environmental Monitoring, 10-15 April 2011, Sydney, Australia, pp. 1–4. ISBN 9780932913142. <https://www.isprs.org/proceedings/2011/ISRSE-34/211104015Final00641.pdf>
- ROUSE, J. W. JR., HAAS, R. H., SCHELL, J. A. and DEERING, D.W. (1974): Monitoring vegetation systems in the Great Plains with ERTS. Third Earth Resources Technology Satellite-1 Symposium- Volume I: Technical Presentations. NASA SP-351, compiled and edited by Stanley C. Freden, Enrico P. Mercanti, and Margaret A. Becker, 1994 p., published by NASA, Washington, D.C., pp. 309–317.
- SALVATORE, M. R., BORGES, S. R., BARRETT, J. E., SOKOL, E. R., STANISH, L. F., POWER, S. N. and MORIN, P. (2020): Remote characterization of photosynthetic communities in the Fryxell basin of Taylor Valley, Antarctica. *Antarctic Science*, 32: 255-270.
- SIEWERT, M. B., OLOFSSON, J. (2020): Scale-dependency of Arctic ecosystem properties revealed by UAV. *Environmental Research Letters*, 15: 129601. doi: 10.1088/1748-9326/aba20b; Erratum: 094030, doi: 10.1088/1748-9326/abcc2b
- SINGH, R., RANJAN, S., NAYAKA, S., PATHRE, U. V. and SHIRKE, P. A. (2013): Functional characteristics of a fruticose type of lichen, *Stereocaulon foliolosum* Nyl. in response to light and water stress. *Acta Physiologiae Plantarum*, 35: 1605-1615.
- STOW, D. A., HOPE, A., MCGUIRE, D., VERBYLA, D., GAMON, J., HUEMMRICH, F., HOUSTON, S., RACINE, C., STURM, M., TAPE, K., HINZMAN, L., YOSHIKAWA, K., TWEEDIE, C., NOYLE, B., SILAPASWAN, C., DOUGLAS, D., GRIFFITH, B., JIA, G., EPSTEIN, H., WALKER, D., DAESCHNER, S., PETERSEN, A., ZHOU, L.M. and MYNENI, R. (2004): Remote sensing of vegetation and land-cover changes in Arctic tundra ecosystems. *Remote Sensing of Environment*, 89: 281-308. doi: 10.1016/j.rse.2003.10.018.
- SOTILLE, M. E., BREMER, U. F., VIEIRA, G., VELHO, L. F., PETSCH, C. and SIMÕES, J. C. (2020): Evaluation of UAV and satellite-derived NDVI to map maritime Antarctic vegetation. *Applied Geography*, 125: 102322.
- TUCKER, C.J. (1979): Red and photographic infrared linear combinations for monitoring vegetation. *Remote Sensing of Environment*, 8: 127-150.

- TURNER, D., LUCIEER, A., MALENOVSKY, Z., KING, D. H. and ROBINSON, S. A. (2014): Spatial co-registration of ultra-high resolution visible, multispectral and thermal images acquired with a micro-UAV over Antarctic moss beds. *Remote Sensing*, 6(5): 4003-4024.
- TURNER, D., LUCIEER, A., MALENOVSKÝ, Z., KING, D. and ROBINSON, S. A. (2018): Assessment of Antarctic moss health from multi-sensor UAS imagery with Random Forest Modelling. *International Journal of Applied Earth Observation and Geoinformation*, 68: 168-179. doi: 10.1016/j.jag.2018.01.004.
- WOEBBECKE, D. M., MEYER, G. E., VON BARGEN, K. and MORTENSEN, D. A. (1995): Color indices for weed identification under various soil, residue, and lighting conditions. *Transactions of the American Society of Agricultural Engineers*, 38(1): 259-269. doi: 10.13031/2013.27838